Appl Phys A (2009) 97: 443–447
DOI 10.1007/s00339-009-5239-6

Applied Physics A
Materials Science & Processing

Magnetic properties and magnetic entropy change in Heusler alloys $Ni_{50}Mn_{35-x}Cu_xSn_{15}$

B. Gao · J. Shen · F.X. Hu · J. Wang · J.R. Sun · B.G. Shen

Received: 21 October 2008 / Accepted: 15 April 2009 / Published online: 2 May 2009

Abstract The influence of Cu substitution for Mn on magnetic properties and magnetic entropy change has been investigated in Heusler alloys, $Ni_{50}Mn_{35-x}Cu_xSn_{15}$ ($x = 2, 5$ and 10). With increasing Cu content from $x = 2$ to $x = 5$, the martensitic transition temperature, T_M, decreases from 220 K to 120 K. Further increasing Cu up to $x = 10$ results in the disappearance of T_M. For samples $Ni_{50}Mn_{33}Cu_2Sn_{15}$ and $Ni_{50}Mn_{30}Cu_5Sn_{15}$, both martensitic and austenitic states exhibit ferromagnetic characteristics, but the magnetization of martensitic phase is notably lower than that of austenitic phase. The magnetization difference, ΔM, across the martensitic transition leads to a considerably large Zeeman energy, $\mu_0 \Delta M \cdot H$, which drives a field-induced metamagnetic transition. Associated with the metamagnetic behavior, a large positive magnetic entropy change ΔS takes place around T_M. For the sample $Ni_{50}Mn_{33}Cu_2Sn_{15}$, ΔS reaches 13.5 J/kg·K under a magnetic field change from 0 to 5 T.

PACS 75.30.Sg · 75.20.En · 75.50.Cc

1 Introduction

Increasing attention has been attracted by magnetocaloric cooling technology due to the recent discoveries of magnetocaloric materials that exhibit a large magnetocaloric effect (MCE) near room temperature. Compared to conventional gas cooling technology, magnetocaloric cooling technology has many advantages such as high efficiency, energy savings and environmental safety. It has been demonstrated that the MCE effect strongly depends on the nature of magnetic transitions in the magnetic materials. A number of compounds such as $Ga_5Si_2Ge_2$ [1], $LaFe_{13-x}Si_x$ [2, 3], $MnAs_{1-x}Sb_x$ [4] and $MnFeP_{1-x}As_x$ [5], Ni-Mn-Ga [6–11], exhibit a large MCE because of the first-order nature of their magnetic transition. Among those materials, an attractive candidate is the Mn-based Heusler alloys.

Since the first report of a large magnetic entropy change associated with the structure transformation in a polycrystalline NiMnGa sample [6], numerous investigations on the magnetic properties and the magnetocaloric effect (MCE) in various ferromagnetic shape memory Heusler alloys (FSMAs) have been carried out [6–11]. For the traditional Heusler alloys, such as Ni-Mn-Ga, the shape memory effect is realized through the field-induced rearrangement of martensite variants. The magnetocaloric effect comes from the magnetization jump caused by the change of magnetic anisotropy upon the martensitic structure transition. In these alloys, the martensitic phase usually shows a higher magnetization than the austenitic phase around the martensitic transition temperature T_M, and the associated ΔS is usually negative according to the Maxwell relation. The recent discovery of metamagnetic shape memory alloys (MSMAs) has stirred intense interest, because of the huge shape memory effect and the different mechanism from the traditional alloys [12]. In these Ga-free Ni-Mn-Z Heusler alloys (where Z can be a group III or group IV element such as In, Sn, or Sb), an excess of Mn makes the martensitic phase exhibit paramagnetic, weaker ferromagnetic, or even antiferromagnetic behavior, while the austenitic phase remains in the strong ferromagnetism regime. Because of the fundamental change of magnetism across the structural transfor-

B. Gao · J. Shen · F.X. Hu (✉) · J. Wang · J.R. Sun · B.G. Shen
State Key Laboratory of Magnetism, Institute of Physics, Chinese Academy of Sciences, Beijing 100190, People's Republic of China
e-mail: hufx@g203.iphy.ac.cn

mation, a field-induced metamagnetic behavior takes place, which is responsible for the huge shape memory effect. The simultaneous change of the structure and magnetic properties induced by a magnetic field should be accompanied by a large MCE. Several groups studied the magnetic properties and magnetic entropy change ΔS in this kind of alloys [11, 13–15]. A large positive ΔS has been observed in $Ni_{50}Mn_{50-x}Sn_x$ ($x = 13, 15$) alloys [11]. The reported ΔS in $Ni_{50}Mn_{35}Sn_{15}$ reaches 14.2 J/kg·K at 187 K under a field change from 0 to 5 T. One knows that the physical properties of Mn-based Heusler alloys can be tunable by adjusting the valence electron concentration, chemical surrounding, as well as the band structure. Their magnetic properties and martensitic transition behaviors can be various, crucially depending on the composition and the corresponding ratio. In this paper, we report on the influence of substitution of Cu for Mn on magnetic properties and magnetic entropy change in $Ni_{50}Mn_{35-x}Cu_xSn_{15}$ ($x = 2, 5$ and 10) alloys.

2 Experimental procedure

Stoichiometric polycrystalline alloys of $Ni_{50}Mn_{35-x}Cu_xSn_{15}$ ($x = 2, 5$, and 10) were prepared by repeatedly arc-melting appropriate amounts of starting materials in high-purity argon atmosphere (99.996%) with a base pressure of 10^{-4} Pa. The commercial purities of Ni, Mn, Cu, Sn are 99.999 wt%, 99.9 wt%, 99.95 wt% and 99.9 wt%, respectively. The obtained ingots were each wrapped with Ta foil and subsequently homogenized in a sealed quartz tube with a high vacuum of 10^{-4} Pa at 1073 K for 72 hours, and then slowly cooled down to room temperature. Samples for measurements were cut from the central parts of each ingot. X-ray diffraction (XRD) measurements on powder of the ingots were performed using Cu Kα radiation to identify the phase and crystal structure. Magnetic measurements were performed using a superconducting quantum interference device (SQUID) magnetometer and a physics property measurement system (PPMS). The magnetic entropy change was evaluated from the isothermal magnetization data using the following Maxwell relation [1–6]:

$$\Delta S_m(T, H) = \int_0^H \left(\frac{\partial M}{\partial T}\right)_H dH. \quad (1)$$

3 Results and discussion

Figure 1 shows X-ray diffraction patterns of samples $Ni_{50}Mn_{35-x}Cu_xSn_{15}$ ($x = 2, 5$ and 10) taken at room temperature. The details around the (220) peak are displayed in the inset of Fig. 1. The clean (220) peak without any splitting for samples with $x = 5$ and 10 indicates that the two samples possess a highly ordered $L2_1$ type structure. For the sample with $x = 2$, a slight distortion of the (220) peak is observed, which may be related to the early stage of the martensitic phase [16]. Because of the very close atomic radius of Mn and Cu, no obvious shift of the diffraction peaks was observed. This result indicates that the lattice constants keep nearly unchanged upon replacing Mn with Cu.

A temperature dependent magnetization under different fields has been measured in zero-field-cooled (ZFC), field-cooled (FC), and field-heated (FH) processes in order to determine magnetic state, transition temperature and the nature of the transitions. The samples were first cooled down to 5 K in zero field; then a magnetic field was applied to the sample and the magnetization was measured on heating with the field fixed, thus the ZFC (heating) magnetization curve was obtained. The FC (cooling) magnetization was measured while cooling the sample to 5 K with the same field, and then the FH (heating) magnetization was obtained on heating under unchanged field. Figure 2 shows the temperature dependent ZFC magnetization (M) under 0.01 T for all samples. As a typical display, the ZFC-FH and ZFC-FC magnetizations under 0.01 T and 1 T for the sample $Ni_{50}Mn_{33}Cu_2Sn_{15}$ are shown in Fig. 3(a) and (b), respectively. One knows that thermal hysteresis is a typical characteristic for the martensitic transition due to the first-order nature of the transition [17], while the magnetic transition at the Curie temperature T_C^A in the austenitic phase shows second-order characteristics (no thermal hysteresis happens around T_C^A). The gap of the thermal hysteresis and the anomaly around 220 K (Fig. 3(b)) suggest the position of the martensitic structural transition, while the anomaly around 310 K indicates the Curie temperature of the austenitic phase. One can find that T_C^A of the austenitic phase is located at 310, 315, and 290 K for samples with $x = 2, 5, 10$,

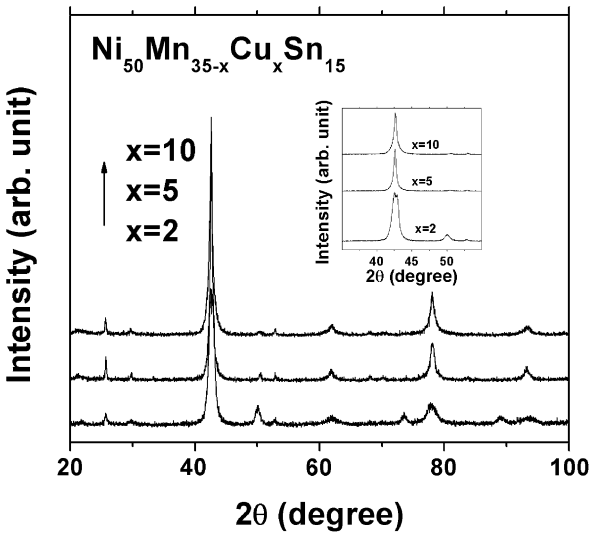

Fig. 1 X-ray diffraction patterns collected at room temperature for $Ni_{50}Mn_{35-x}Cu_xSn_{15}$ ($x = 2, 5$, and 10) alloys. The inset exhibits the details around (220) peak

respectively. With decreasing temperature a lattice instability appears. The samples transform to martensitic phase at the martensitic transformation temperature (T_M). T_M is located at 220 K and 120 K for the samples $Ni_{50}Mn_{33}Cu_2Sn_{15}$ and $Ni_{50}Mn_{30}Cu_5Sn_{15}$, respectively. Further increasing Cu up to $x = 10$ results in a disappearance of the martensitic transition. The sample $Ni_{50}Mn_{25}Cu_{10}Sn_{15}$ preserves a cubic structure in the whole measured temperature range from 5 to 350 K. The width of the thermal hysteresis around T_M is about 12 K for the $Ni_{50}Mn_{33}Cu_2Sn_{15}$ sample (see Fig. 3(b)). In the low temperature range in martensitic states, a large separation between ZFC and FH magnetization is observed under a low field of 0.01 T (Fig. 3(a)) for $Ni_{50}Mn_{33}Cu_2Sn_{15}$ and $Ni_{50}Mn_{30}Cu_5Sn_{15}$ samples, which can be understood by considering the magnetic anisotropy in the martensitic state [18, 19] (no hysteresis was observed around T_M in Fig. 3(a) because the magnetization in both ZFC and FH process is collected on heating). The reduced structural symmetry enhanced the magnetic anisotropy. An external cooling field could govern the magnetic domain configuration, resulting in the splitting between ZFC and FH magnetization.

With increasing Cu content from $x = 2$ to $x = 5$, T_M drops from 220 to 120 K, while T_C^A slightly increases. One knows that the valence electron concentration, e/a (i.e. valence electrons per atom), is a critical factor that influences the characteristics of ferromagnetic Heusler alloys. It has been well established that the compositional dependence of T_M is related to e/a. When the Fermi surface reaches the Brillouin zone boundary, structural instabilities appear and a martensitic transition takes place [20]. The change in the number of valence electrons and the alteration of the Brillouin zone boundary are considered to be the driving forces for the occurrence of the martensitic structural transformation. The valence electron concentrations of the present $Ni_{50}Mn_{35-x}Cu_xSn_{15}$ were calculated by using the electron configurations of the outer shells for each element. i.e. Ni, $3d^84s^2$-10; Mn, $3d^54s^2$-7; Cu, $3d^{10}4s^1$-11; Sn, $5S^25P^2$-4. The obtained value of e/a is 8.05, 8.13, 8.25 and 8.45 for $x = 0, 2, 5$ and 10, respectively. The e/a-dependence of T_M was found to increase monotonously in many NiMn-based ternary or quaternary Heusler alloys [21]. However, for present $Ni_{50}Mn_{35-x}Cu_xSn_{15}$, a nonmonotonic dependence of T_M on e/a was found. According to [11], T_M is located at 187 K for sample $Ni_{50}Mn_{35}Sn_{15}$ (e/a $\sim$ 8.05) without Cu. When e/a reaches 8.13 ($x = 2$), T_M increases to 220 K, which is in agreement with the general dependence of T_M on e/a. However, with further increasing e/a to 8.25 ($x = 5$) T_M does not continuously increase but sharply drops to 120 K. As e/a reaches 8.45 ($x = 10$), T_M completely disappears. Obviously, the simple rule between e/a and T_M does not fit the present systems. The following possible reasons were considered for the unusual observations. One is that the general relation between T_M and e/a may lose effectiveness when e/a approaches 8.5 (the case of $Ni_{50}Mn_{50}$); another is the question of the number of valence electrons for element Cu. The electron configuration of Cu is $3d^{10}4s^1$. Some people chose only the 4s electron,

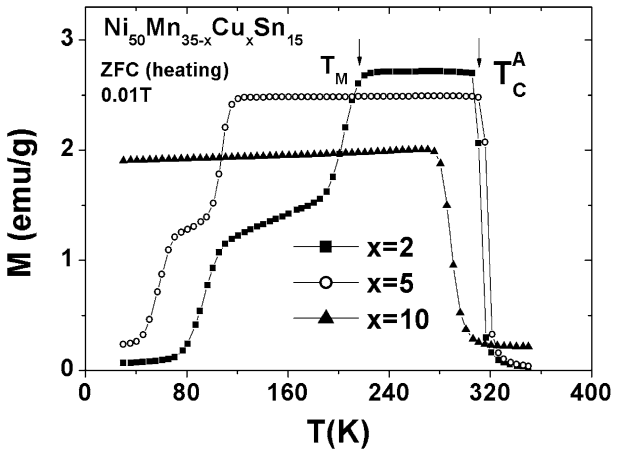

Fig. 2 Temperature dependent ZFC (heating) magnetization measured under 0.01 T magnetic field for samples $Ni_{50}Mn_{35-x}Cu_xSn_{15}$ ($x = 2, 5$, and 10)

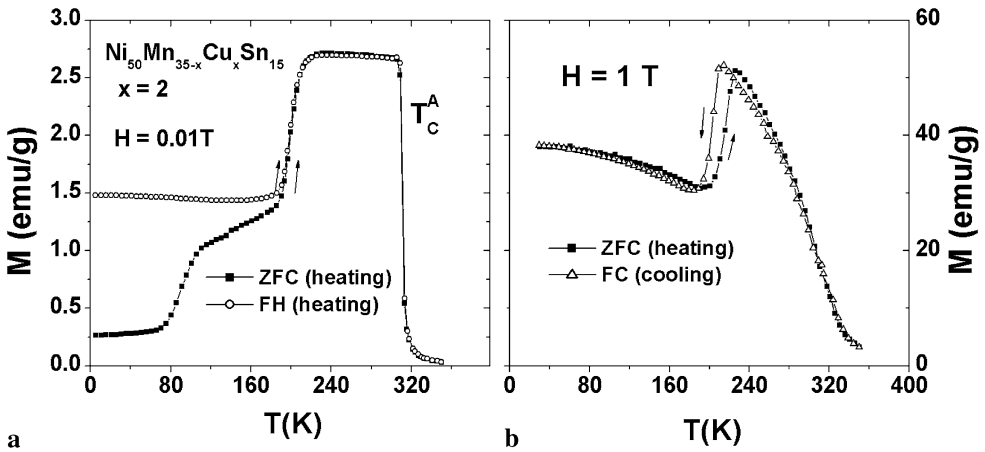

Fig. 3 (**a**) ZFC (heating) and FH (heating) magnetization measured under 0.01 T, and (**b**) ZFC (heating) and FC (cooling) magnetization measured under 1 T for sample $Ni_{50}Mn_{33}Cu_2Sn_{15}$

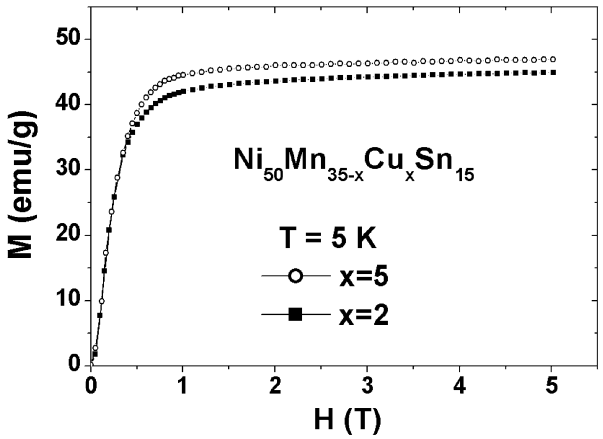

Fig. 4 Magnetization as a function of magnetic field (M–H) at 5 K for samples $Ni_{50}Mn_{35-x}Cu_xSn_{15}$ ($x = 2, 5$)

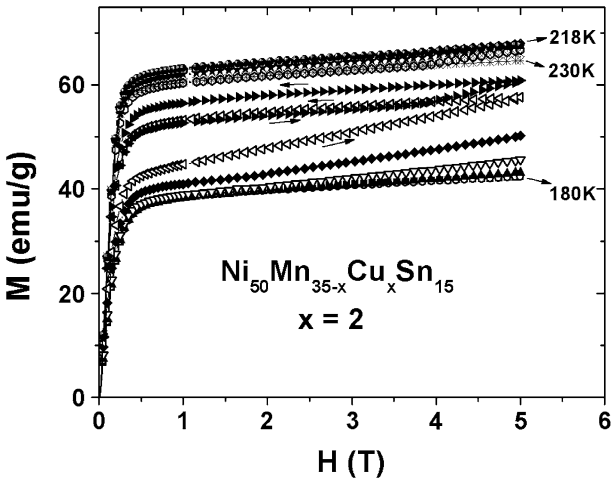

Fig. 5 Magnetization isotherms (M–H) for $Ni_{50}Mn_{33}Cu_2Sn_{15}$ alloy at temperatures around T_M. For the sake of clarity, the magnetization loop on field increase and decrease is presented only for temperatures close to T_M. The other M–H curves are on field increase

i.e. 1 electron, as the valence electron of Cu [22], while others used both 3d and 4s electrons, i.e. 11 [23, 24]. The actual number of valence electrons contributed by Cu should depend on the chemical environments in specific compounds. Similar to our observations, an opposite dependence of T_M on e/a is also observed in $Ni_{2-x}Cu_xMnGa$ alloys [24], in which T_M decreases with e/a increasing on the assumption that valence electrons of Cu is 11. Finally, the structure as well as the crystallographic symmetry is considered to be another essential factor influencing T_M. Any subtle change in the crystal structure would affect electronic structure and thus the martensitic transition behavior. Recent investigations [25] indicated that in NiMn-based Heusler alloys with an excess of Mn, the replacement of Mn by Co would break the crystallographic symmetry and cause an aligned ferromagnetic order between Mn atoms and thus an enhancement of magnetization. The exchange coupling is suggested to be a competition between the spin polarization of transportation electrons among localized Mn moments and the s-p hybridizing effect entailed by Co. However, for the samples with Cu coping, because the Ni atom is larger than Cu but smaller than Mn, the addition of Cu may substitute Ni partially and some of the Ni atoms have to occupy Mn positions. As a result, Cu-doping may have a different influence on the electronic structure compared with Co-doping, and thus a complex e/a-dependence can be observed.

Shown in Fig. 4 is the magnetization as a function of the magnetic field (M–H) collected at 5 K for samples $x = 2$, and 5. One can find that the martensitic phase exhibits ferromagnetic behaviors for both samples. The magnetization is nearly saturated when H reaches 1 T. Around T_M, the magnetization of the martensitic phase is still lower than that of the austenitic phase (see Fig. 3(b)). The magnetization difference ΔM across the martensitic transition will lead to a considerable large Zeeman energy, $\mu_0 \Delta M \cdot H$, which drives a field-induced metamagnetic transition.

Figure 5 displays the magnetization isotherms (M–H) measured at temperatures around T_M for sample $x = 2$. For the sake of clarity, the magnetization loop on field increase and decrease is presented only for the temperatures close to T_M. The other M–H curves are on field increase. The upturn in the curves below but near T_M is associated with the field-induced metamagnetic behavior, accompanied by a structural transition from the martensitic to austenitic state. The nature of low magnetization in the martensitic state may come from the contribution of the Mn–Mn antiferromagnetic coupling. In the stoichiometric Ni_2Mn-based Heusler alloys, such as Ni_2MnGa, Ni_2MnIn, and Ni_2MnSn, the nearest neighboring distance between the Mn atoms is around 0.4 nm. RKKY exchange through conductive electrons leads to a ferromagnetic ordering. The magnetization is mainly confined to Mn atoms, $\sim 4.0 \mu_B$. However, in the off-stoichiometric alloys with an excess of Mn, the nearest distance between Mn atoms is suddenly changed to a small value and antiferromagnetic Mn–Mn alignment appears. The competition between ferromagnetic and antiferromagnetic coupling leads to the weaker ferromagnetism of the martensitic state.

The magnetic entropy change $\Delta S(T, H)$ is calculated based on the Maxwell relation shown in (1). Figure 6 displays ΔS as a function of temperature under different fields for the sample with $x = 2$. One can find that the ΔS is positive and peaks at T_M (220 K). The maximum of ΔS reaches 13.5 J/kg·K under a magnetic field change from 0 to 5 T. One can note that the peak value of ΔS for $Ni_{50}Mn_{33}Cu_2Sn_{15}$ has a magnitude comparable with that of the undoped alloy $Ni_{50}Mn_{35}Sn_{15}$($\Delta S \sim 14.2$ J/kg·K, $T_M \sim 187$ K) [11], but is located at a higher temperature range. The Cu-doped compounds may be useful as magnetic refrigerants in the corresponding temperature range.

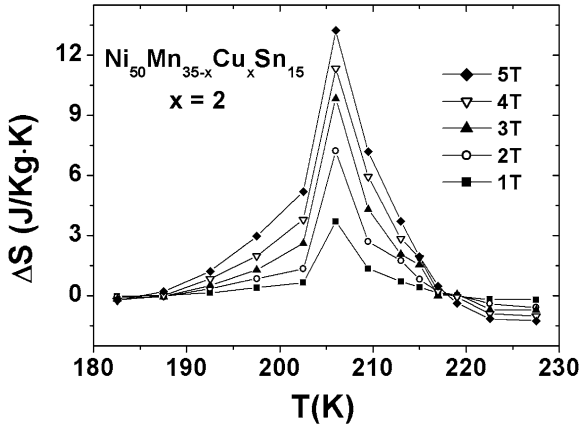

Fig. 6 Magnetic entropy change ΔS as a function of temperature under different magnetic fields for sample $Ni_{50}Mn_{33}Cu_2Sn_{15}$

4 Conclusion

In summary, we investigated the influence of the substitution of Cu for Mn on magnetic properties and magnetic entropy change in $Ni_{50}Mn_{35-x}Cu_xSn_{15}$ alloys. It was found that the martensitic transition behaviors and magnetic properties are sensitive to the Cu content. When x increases from $x = 2$ to 5, the martensitic transition temperature T_M drops from 220 K to 120 K, while the Curie temperature T_C^A of the austenitic state slightly increases. Furthermore, martensitic transition behavior completely disappears when the Cu content reaches $x = 10$. The dependence of T_M on the valence electron concentration, e/a, is not monotonous for the present systems. Possible reasons are discussed. Around T_M, the martensitic phase shows weaker ferromagnetic properties than the austenitic phase, which leads to a positive magnetic entropy change ΔS. The ΔS for sample $x = 2$ reaches 13.5 J/kg·K under a magnetic field change from 0 to 5 T, which is comparable with that of the undoped $Ni_{50}Mn_{35}Sn_{15}$ but is located at a higher temperature range.

Acknowledgements This work has been supported by the National Natural Science Foundation of China, Hi-Tech Research and Development program of China, the Knowledge Innovation Project of the Chinese Academy of Sciences, and the National Basic Research of China.

References

1. V.K. Pecharsky, K.A. Gschneidner Jr., Phys. Rev. Lett. **78**, 4494 (1997)
2. F.X. Hu, B.G. Shen, J.R. Sun, Z.H. Cheng, G.H. Rao, X.X. Zhang, Appl. Phys. Lett. **78**, 3675 (2001)
3. F.X. Hu, B.G. Shen, J.R. Sun, X.X. Zhang, Chin. Phys. **9**, 550 (2000)
4. H. Wada, Y. Tanabe, Appl. Phys. Lett. **79**, 3302 (2001)
5. O. Tegus, E. Brück, K.H.J. Buschow, F.R. de Boer, Nature **415**, 150 (2002)
6. F.X. Hu, B.G. Shen, J.R. Sun, Appl. Phys. Lett. **76**, 3460 (2000)
7. F.X. Hu, B.G. Shen, J.R. Sun, G.H. Wu, Phys. Rev. B **64**, 132412 (2001)
8. J. Marcos, L. Mañosa, A. Planes, F. Casanova, X. Batlle, A. Labarta, Phys. Rev. B **68**, 094401 (2003)
9. S. Stadler, M. Khan, J. Mitchell, N. Ali, A.M. Gomes, I. Dubenko, A.Y. Takeuchi, A.P. Guimarães, Appl. Phys. Lett. **88**, 192511 (2006)
10. M. Pasquale, C.P. Sasso, L.H. Lewis, L. Giudici, T. Lograsso, D. Schlagel, Phys. Rev. B **72**, 094435 (2005)
11. T. Krenke, E. Duman, M. Acet, E.F. Wassermann, X. Moya, L. Mañosa, A. Planes, Nat. Mater. **4**, 450 (2005)
12. R. Kainuma, Y. Imano, W. Ito, Y. Sutou, H. Morito, S. Okamoto, O. Kitakami, K. Oikawa, A. Fujita, T. Kanomata, K. Ishida, Nature **439**, 957 (2006)
13. T. Krenke, E. Duman, M. Acet, E.F. Wassermann, X. Moya, L. Mañosa, A. Planes, E. Suard, B. Ouladdiaf, Phys. Rev. B **75**, 104414 (2007)
14. Z.D. Han, D.H. Wang, C.L. Zhang, S.L. Tang, B.X. Gu, Y.W. Du, Appl. Phys. Lett. **89**, 182507 (2006)
15. V.K. Sharma, M.K. Chattopadhyay, R. Kumar, T. Ganguli, P. Tiwari, S.B. Roy, J. Phys.: Condens. Matter **19**, 496207 (2007)
16. M. Khan, I. Dubenko, S. Stadler, N. Ali, J. Appl. Phys. **97**, 10M304 (2005)
17. J. Ortin, L. Delaey, Int. J. Non-Liner Mech. **37**, 1275 (2002)
18. T. Krenke, M. Acet, E. Wassermann, X. Moya, L. Mañosa, A. Planes, Phys. Rev. B **73**, 174413 (2006)
19. S.-Y. Chu, A. Cramb, M. De Graef, D. Laughlin, M.E. McHenry, J. Appl. Phys. **87**, 5777 (2000)
20. P.J. Webster, K.R.A. Ziebeck, S.L. Town, M.S. Peak, Philos. Mag. B **49**, 295 (1984)
21. V.A. Cherneko, E. Cesari, V.V. Kokorin, I.N. Vitenko, Scr. Metall. Mater. **33**, 1239 (1995)
22. E. Obrado, L. Manosa, A. Planes, Phys. Rev. B **56**, 20 (1997)
23. B.R. Gautam, I. Dubenko, J.C. Mabonl, S. Stadler, N. Ali, J. Alloys Compd. **472**, 35 (2009)
24. T. Kanomata, T. Nozawa, D. Kikuchi, H. Nishihara, K. Koyama, K. Watanabe, Int. J. Appl. Electromagn. Mech. **21**, 151 (2005)
25. L. Ma, H.W. Zhang, S.Y. Yu, Z.Y. Zhu, J.L. Chen, G.H. Wu, H.Y. Liu, J.P. Qu, Y.X. Li, Appl. Phys. Lett. **92**, 032509 (2008)